

CutS3D: Cutting Semantics in 3D for 2D Unsupervised Instance Segmentation

Leon Sick
Ulm University

Dominik Engel
Ulm University

Sebastian Hartwig
Ulm University

Pedro Hermosilla
TU Vienna

Timo Ropinski
Ulm University

Abstract

Traditionally, algorithms that learn to segment object instances in 2D images have heavily relied on large amounts of human-annotated data. Only recently, novel approaches have emerged tackling this problem in an unsupervised fashion. Generally, these approaches first generate pseudo-masks and then train a class-agnostic detector. While such methods deliver the current state of the art, they often fail to correctly separate instances overlapping in 2D image space since only semantics are considered. To tackle this issue, we instead propose to cut the semantic masks in 3D to obtain the final 2D instances by utilizing a point cloud representation of the scene. Furthermore, we derive a Spatial Importance function, which we use to resharpen the semantics along the 3D borders of instances. Nevertheless, these pseudo-masks are still subject to mask ambiguity. To address this issue, we further propose to augment the training of a class-agnostic detector with three Spatial Confidence components aiming to isolate a clean learning signal. With these contributions, our approach outperforms competing methods across multiple standard benchmarks for unsupervised instance segmentation and object detection.

1. Introduction

Localizing and segmenting instances in natural images has long been considered a challenging task in computer vision. In recent years however, supervised algorithms [4, 8, 9, 19, 21, 37, 49] have made impressive progress towards enabling the segmentation of a large diversity of objects in a variety of environments and domains. But for these supervised models to perform well, they require a large amount of labeled training data, which, especially for instance segmentation, is costly to obtain, since annotations for instance segmentation have to contain information about individual instances of a particular class. One prominent example is the COCO dataset [27], containing around 164 thousand

images with instance mask annotations distributed across 80 classes, which required more than 28 thousand hours of annotation time across a large group of labelers. This enormous effort has sparked the field of unsupervised instance segmentation, which aims to develop algorithms that can perform such segmentations with similar quality, but without needing any human annotations used during training. CutLER, a recent approach by Wang et al. [47], has made significant progress in unsupervised instance segmentation of natural scenes by training a class-agnostic detection network (CAD) on pseudo-masks generated by MaskCut. To do so, the authors leverage self-supervised features to capture the 2D semantics of the scene in an affinity graph and extract instance pseudo-masks. However, since their approach only considers semantic relations, it fails to separate instances of the same class that are overlapping or connected in 2D space. In contrast, humans inherently perceive the natural world in 3D, an ability which helps them to better separate instances by not just considering visual similarity, but also their boundaries in 3D. Nowadays, precise 3D information is readily available through zero-shot monocular depth estimators trained solely with sensor data and no human annotations, thus not breaking the unsupervised setting. Further, previous work has already shown that using spatial information is helpful for unsupervised semantic segmentation [39]. We argue that, in order to separate instances effectively, information about the 3D geometry of the scene also needs to be taken into account.

Within this work, we propose **CutS3D (Cutting Semantics in 3D)**, the first approach to introduce 3D information to separate instances from semantics for 2D unsupervised instance segmentation. **CutS3D** effectively incorporates this 3D information in various stages: For pseudo-mask extraction, we go beyond 2D separation and cut instances in 3D. Starting from an initial semantics-based segmentation, we cut the object along its actual 3D boundaries from a point cloud of the scene, obtained by orthographically projecting the depth map. To 3D-align the feature-

based affinity graph for the initial semantic cut, we further compute a Spatial Importance function which assigns a high importance to regions with high-frequency depth changes. The Spatial Importance map is then used to sharpen the semantic affinity graph, effectively enriching it with 3D information in order to make cuts along object boundaries more likely. While the generated pseudo ground truth is useful to train the CAD, these pseudo mask are inherently ambiguous. We therefore again leverage 3D information to extract information about the quality of the pseudo-masks at individual patches to separate clean from potentially noisy learning signals. To achieve this, we introduce Spatial Confidence maps which are computed by performing multiple 3D cuts at different scales. We argue this captures the confidence the algorithm has in the instance separation along the spatial boundaries, since we observe that only for objects with unclear boundaries, these cuts yields slightly different results at varying scales. We leverage these Spatial Confidence maps in three ways when training the CAD. First, we select only the highest-confidence masks within an image for copy-paste augmentation. Second, we perform alpha-blending so that object regions are blended with the current image proportionally to their region confidence. Third, we use our Spatial Confidence maps to introduce a Spatial Confidence Soft Target loss, a more precise way to incorporate the signal quality in the mask loss. In summary, we propose the following contributions:

1. **LocalCut** to cut objects along their actual 3D boundaries based on an initial semantic mask.
2. **Spatial Importance Sharpening** for 3D-infusing the semantic graph to better represent 3D object boundaries.
3. **Spatial Confidence** that captures pseudo-mask quality to select only **confident masks** for copy-paste augmentation, **alpha-blend** instances when copy-pasting, and introduce a novel **Spatial Confidence Soft Target Loss**.

2. Related Work

Self-Supervised Representation Learning. The advances of self-supervised feature learning, which aims to propose methods for learning deep features without human annotations or supervision, have been central to significant progress in unsupervised instance segmentation. One popular approach, DINO by Caron et al. [6], employs a student-teacher learning process with cropped images to make a ViT learn useful features. Their work has been demonstrated to produce semantically relevant features and attention maps, and has been employed by various approaches in unsupervised segmentation [1, 17, 23, 26, 35, 39, 40, 47]. In their work on MoCo, He et al. [20] use contrastive learning to produce meaningful representations through the use of a momentum encoder and achieve a more scalable and efficient pre-training process. DenseCL, proposed by Wang et al. [44], also utilizes contrastive learning, but with the spe-

cific goal of learning representations useful for dense prediction and introduce a pairwise pixel-level similarity loss between image views. Oquab et al. [30] propose DINO’s successor, called DINOv2, by introducing optimizations such as KoLeo regularization [34], Sinkhorn-Knopp centering [5] or the patch-level objective from iBOT [50]. Another recent follow-up to DINO is proposed by Lui et al. [28] with DiffNCuts. They implement a differentiable version of Normalized Cuts (NCut) and use a mask consistency objective on cuts from different image crops to finetune a DINO model. After training, they show that their model improves upon vanilla DINO for object discovery tasks.

Unsupervised Instance Segmentation. Recent progress in unsupervised instance segmentation has been accelerating rapidly. LOST [40] extracts DINO features to identify a seed patch with minimal similarity from an image, then expands it based on patch similarities to create object masks. MaskDistill [43] uses a bottom-up approach and leverages a pixel grouping prior from MoCo features to extract masks, which serve as input to training a Mask R-CNN [19]. In contrast, FreeSOLO [46] uses features from DenseCL as part of a key-query design to extract query-informed attention maps that represent masks. These are further used as pseudo masks to train a SOLO model [45]. Wang et al. [47] propose CutLER by extending an NCut-based mask extraction process from DINO features, first proposed by TokenCut [48], to the multi-instance case. After extracting pseudo-masks with MaskCut, they train a detection network for multiple rounds on its own predictions. We provide a more detailed description of CutLER in Section 3.1. CuVLER by Arica et al. [1] also follows this approach, but uses an ensemble of 6 DINO models to extract pseudo-masks, as well as a soft target loss to incorporate a confidence score into the training of the detector. Finally, Li et al. take a different approach with ProMerge [26] and attempt to identify the background of the scene in combination with point prompting to then sequentially segment and merge individual instances. Further, they also train a detection network on the generated instance masks.

3. Method

We build upon CutLER [47] and first extract pseudo-masks to then train a CAD on the generated pseudo ground thruth. We introduce LocalCut (Sec. 3.2) and Spatial Importance Sharpening (Sec. 3.3) for pseudo-mask extraction, as well as three Spatial Confidence components (Sec. 3.4) for training the CAD.

3.1. Preliminaries

Following Wang et al. [47], we first feed the input image through a DINO [6] Vision Transformer (ViT) [11] $\mathcal{F} : \mathbb{R}^{3 \times H_{in} \times W_{in}} \rightarrow \mathbb{R}^{C \times H \times W}$ to extract a feature map $f \in \mathbb{R}^{C \times H \times W}$. Afterwards, we calculate a semantic affinity

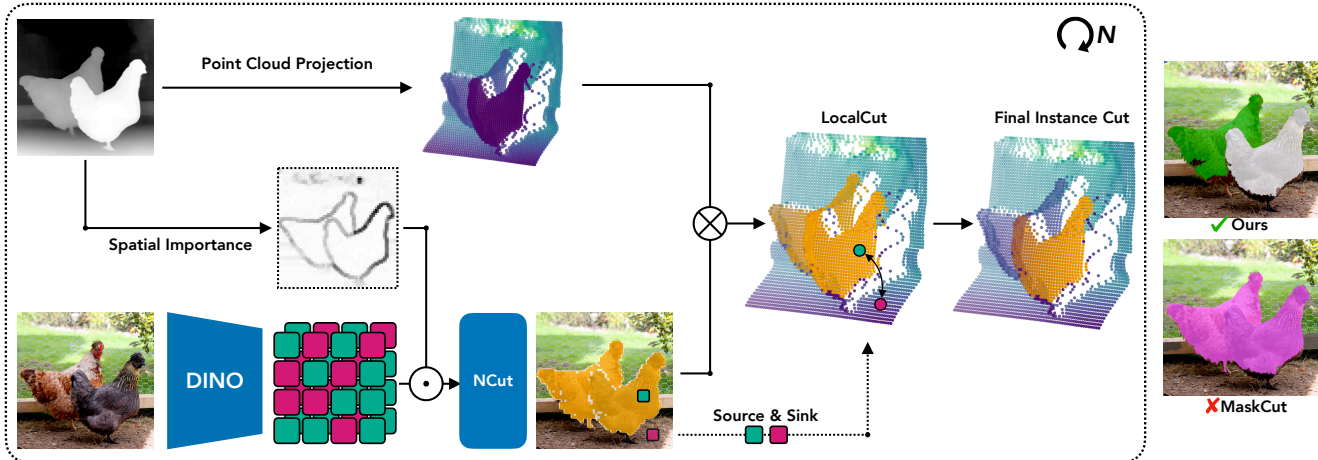


Figure 1. **CutS3D Pseudo-Mask Extraction Pipeline.** We separate instances in 3D, cutting semantics groups into instances even if they are connected in 2D space. To make the semantic affinity matrix 3D-aware, we sharpen it using Spatial Importance maps to improve the semantic relations along the 3D boundaries of instances.

matrix $W_{i,j} = \frac{f_i \cdot f_j}{\|f_i\|_2 \|f_j\|_2}$. This affinity matrix represents a fully-connected undirected graph, i.e., an affinity graph, with cosine similarities as edge weights, on which we apply Normalized Cuts (NCut) [38] by solving $(Z-W)x = \lambda Zx$, where Z is a $K \times K$ diagonal matrix with $z(i) = \sum_j W_{i,j}$. The goal of NCut is to find the eigenvector x that matches the second smallest eigenvalue λ . The algorithm yields an eigenvalue decomposition of the graph, i.e., we obtain an eigenvalue for each node. This defines $\lambda_{\max} = \max_e |\lambda_e|$ as the semantically most forward and $\lambda_{\min} = \min_e |\lambda_e|$ as the semantically most backward point. MaskCut [47] binarizes the graph with the threshold τ^{ncut} and cuts a bipartition B from the graph, a process which is repeated for N segmentation iterations per image. Our approach leverages this semantic bipartition as an initial semantic mask. After each cut, we remove the nodes corresponding to the previously obtained segmentation from the affinity graph. We find that in some cases, all objects in the scene are assigned an instance after $n < N$ iterations. This is indicated by the algorithm predicting the inverse of all previous segmentation masks combined, i.e., it predicts the "rest". If this occurs, we stop our pseudo-mask extraction for this image.

3.2. LocalCut: Cutting Instances in 3D

To identify the most relevant semantic group of the scene, NCut relies on global semantic information of the scene, represented by the feature-based affinity graph. We argue that, to separate individual instances from a semantic group, local information is most effective. While the naive 2D connected component filter in MaskCut [47] takes into account local properties, it can fail to identify the actual instance boundaries if the instances are connected in 2D and semantically similar. We overcome this issue by leveraging 3D information in the form of a point cloud to segment in-

stances along their actual boundaries in 3D space, which we illustrate in Figure 1. To achieve this, we first extract a depth map $D \in [0, 1]$ from the input image using an off-the-shelf zero-shot monocular depth estimator, in this case ZoeDepth [2]. We adapt this depth map to the resolution of the patch-level feature map f , and unproject it orthographically into a point cloud P , consisting of a set of points $\{p_1, p_2, \dots, p_m\}$. We leverage the previously described initial semantic bipartition B and only keep points that are part of this initial semantic cut. To capture the local geometric properties of the 3D space, we construct a k -NN graph $G^{3D} = (V, E)$ on this pre-filtered point cloud with the edge e being assigned a weight c , the Euclidean distance between two points. This graph is effective for capturing local geometric structures within the semantic region, since a given point is only connected to its k closest neighbors in 3D space. We then thresholding the graph with τ_{knn} and cut the instance from the semantic mask in 3D using MinCut on the point cloud [15]. MinCut aims to partition the graph into two disjoint subsets by minimizing the overall edge weights that need to be removed from the graph. More specifically, we use an implementation of Dinic’s algorithm [10] to solve the maximum-flow problem, whose objective to maximize the total flow from the source node to the sink node is equal to the MinCut objective. For the algorithm to produce the desired output, source s shall be set to the most foreground point and sink t to the most background point. We exploit these two parameters to effectively connect the semantic space to the 3D space: Instead of the defining foreground and background by analyzing the point cloud, we leverage information obtained through NCut on the semantic affinity graph and set $s = p_{\lambda_{\max}}$, i.e. the point at the maximum absolute eigenvalue, and $t = p_{\lambda_{\min}}$, i.e. the point at the minimum absolute eigenvalue. By definition, these are



Figure 2. **Visualization of CutS3D Pseudo-Masks.** We showcase the capability of our pseudo-mask extraction pipeline. Our method is able to separate instances in 3D space, enabling the separating of same-class instances such as the humans playing tennis on the left. MaskCut [47] only takes into account 2D, therefore it fails to separate the humans positioned behind each other.

the points selected by NCut from the semantic space to be foreground and background. Like MaskCut [47], this mask is then further refined with a Conditional Random Field (CRF) [24]. We display a selection of generated pseudo-masks in Figure 2.

3.3. Spatial Importance Sharpening

As previously described, we partition the point cloud with a semantic mask as the basis for our LocalCut. To obtain this semantic mask in the first place, NCut [38] aims to find the most relevant region on the fully-connected semantic graph so that the similarity within this region is maximized and the similarity between different regions is minimized. Since we can exploit 3D information of the scene, we propose to enrich the semantic graph and make it 3D-aware. We observe that the semantic cut can generate masks that do not fully capture the instance boundary, missing parts of the instance that are important for accurate segmentation. With the intuition that our LocalCut will profit from an improved semantic mask, we aim to sharpen the semantic similarities along the object border since we want to include the spatially important areas of the object in the semantic mask for LocalCut to find the accurate 3D boundary. If this region is not part of the mask, LocalCut will not be able to cut at the 3D boundary. To achieve this, we first compute a Spatial Importance map based on the available depth. The goal is to assign high Spatial Importance values to regions with high-frequency components, since those areas contain important information about where the actual object boundaries might be located. We take inspiration from work by Luft et al. [29] who introduce Spatial Importance as part of an unsharp masking technique for image enhancement. A Gaussian low-pass filter G_σ is used to smooth out the high-frequency components. We apply Gaussian blurring to the

depth map and subtract the original depth map to obtain the Spatial Importance ΔD :

$$\Delta D = |G_\sigma * D - D| \quad (1)$$

where $G_\sigma * D$ denotes convolution with the Gaussian kernel. Further, we normalize ΔD to be in $\in [\beta, 1.0]$:

$$\Delta D_n = \frac{(1.0 - \beta) \cdot (\Delta D - \min \Delta D)}{(\max \Delta D - \min \Delta D)} + \beta \quad (2)$$

To now infuse our semantic affinity matrix with 3D, we re-sharpen the individual cosine similarities using with element-wise exponentiation

$$W_{i,j} = W_{i,j}^{1 - \Delta D_{n,i,j}}, \quad \text{for } i, j = 1, \dots, N. \quad (3)$$

Subtracting the original depth from the blurred depth reveals areas with rapid depth changes which have a high likelihood of representing a 3D object boundary. We set the lower bound $\beta = 0.45$ based on empirical findings. This is to sharpen importance of semantic similarities at object boundaries. In our ablation in Table 4, we show that this step to sharpen similarities in areas of high Spatial Importance in combination with LocalCut, which now can cut at the actual 3D boundary, leads to a significant boost in performance. We ablate β in the supplementary.

3.4. Spatial Confidence

While the generated pseudo-masks provide a useful learning signal, we make a similar observation as Wang et al. [47], that these masks profit from further processing to create a 'cleaner' signal. We also adopt their proposed solution of training a CAD on these pseudo-masks. To improve on this process, we further propose to extract information

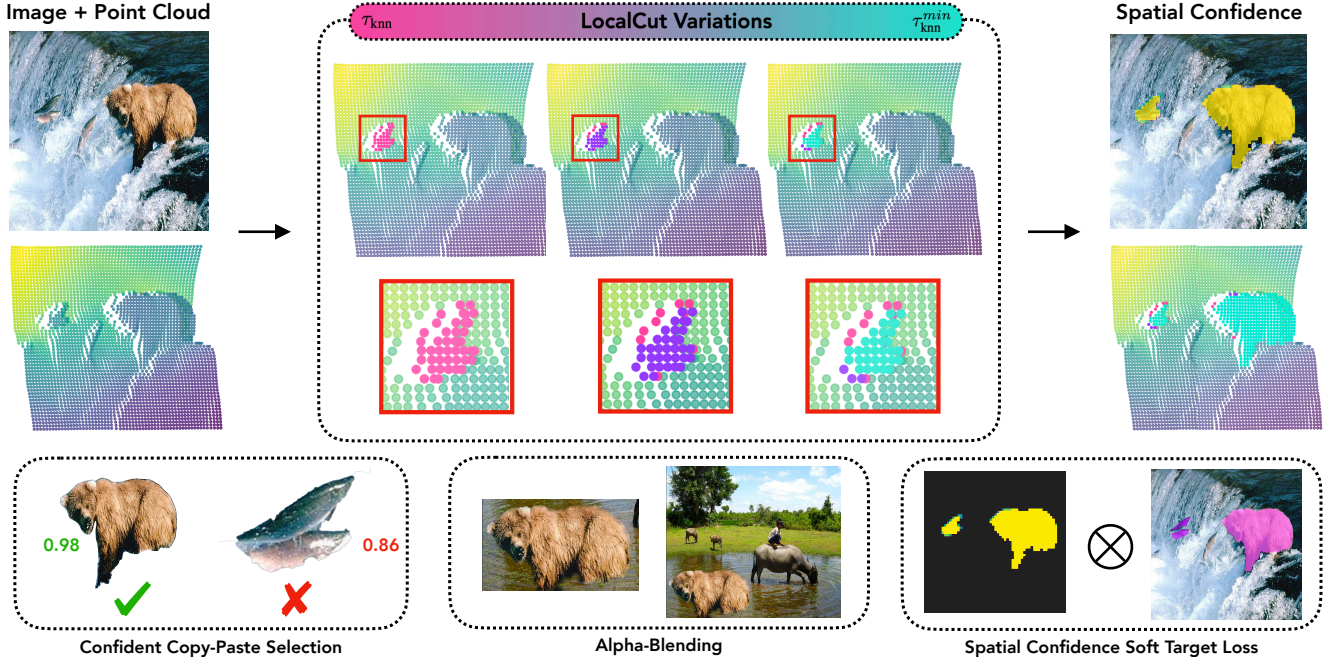


Figure 3. **Spatial Confidence Process.** We introduce Spatial Confidence maps to capture the quality of the 3D-semantic pseudo-mask extraction process. For this, we compute multiple cuts on the points cloud by varying τ_{knn} , then accumulate and average the different masks. We use our Spatial Confidence for selecting confident masks and applying alpha-blending for copy-paste augmentation, as well as introducing a novel Spatial Confidence Soft Target Loss.

about the quality of the pseudo-masks using our 3D information. Specifically, we compute Spatial Confidence maps, which aim to capture the certainty of the individual patches within the final 3D cut. Figure 3 displays our process.

A central LocalCut parameter is the threshold τ_{knn} . We observe that for objects with well-separated 3D boundaries, this parameter is insensitive and produces the same final mask at different values. In contrast, when the 3D boundary of the object is not well defined, the resulting segmentation mask will vary. We exploit this property to compute Spatial Confidence maps in an attempt to capture the quality of a given pseudo-mask, especially along its boundaries. To compute the Spatial Confidence map SC for a given instance, we linearly sample T variations between τ_{knn}^{min} and τ_{knn} to perform LocalCut for each configuration. The resulting binary cuts BC are accumulated and averaged to obtain the Spatial Confidence SC:

$$SC_{i,j} = \frac{1}{T} \sum_{t=1}^T BC_{i,j}(t) \quad (4)$$

We set the minimum confidence SC_{ij}^{min} in the map to 0.5 and ablate this parameter in Table 5c. We generate a Spatial Confidence map for each generated pseudo-mask and utilize it in three different ways during the CAD training.

Confident Copy-Paste Selection. Copy-paste augmentation [14] has been shown to be effective for training the

CAD on the pseudo-masks [47]. Therefore, we opt to also use this augmentation when training our model, but with a twist: Instead of randomly choosing which masks to copy, we select only the highest quality masks, as determined by our Spatial Confidence maps, to be augmented. For this, we average the confidence scores for the entire mask into a single score and use it to sort the masks within an image. This reduces the amount of ambiguous masks which are copied, leading to better performance as shown in Table 4.

Confidence Alpha-Blending. We experiment with including alpha-blending augmentation when copy-pasting object masks. Standard copy-paste augmentation uses a binary mask to paste the selected object into a different image or location. Instead, we again make use of our Spatial Confidence mask to alpha-blend the uncertain regions of the object into the new image I^{aug} , making pixels i, j partially transparent proportional to their confidence

$$I_{i,j}^{aug} = SC_{i,j} \cdot I_{i,j}^S + (1 - SC_{i,j}) \cdot I_{i,j}^T \quad (5)$$

with I^S being the source image from which the object is copied and I^T being the target image to-be-pasted-in. We set $SC_{i,j} = 0$ for regions other than the copied instance. For areas with high confidence, the object is fully pasted, whereas the pixel values for regions with lower confidence are blended with those of the image that they are pasted into. Combined with the confidence-based mask selection, we observe this further improves performance.

Method	Backbone	COCO20K						COCOval2017					
		AP ₅₀ ^{box}	AP ₇₅ ^{box}	AP ^{box}	AP ₅₀ ^{mask}	AP ₇₅ ^{mask}	AP ^{mask}	AP ₅₀ ^{box}	AP ₇₅ ^{box}	AP ^{box}	AP ₅₀ ^{mask}	AP ₇₅ ^{mask}	AP ^{mask}
LOST [40]	DINO	-	-	-	2.4	1.0	1.1	-	-	-	-	-	-
MaskDistill [43]	MoCo	-	-	-	6.8	2.1	2.9	-	-	-	-	-	-
FreeSOLO [46]	DenseCL	9.7	3.2	4.1	9.7	3.4	4.3	9.6	3.1	4.2	9.4	3.3	4.3
ProMerge+ [26]	DINO	-	-	-	-	-	9.0	-	-	-	-	-	8.9
CutLER [47]	DINO	22.4	11.9	12.5	19.6	9.2	10.0	21.9	11.8	12.3	18.9	9.2	9.7
CuVLER* [1]	DINO	23.5	11.9	12.7	20.0	9.0	10.0	23.0	11.8	12.6	19.3	8.8	9.8
CutS3D (Ours)	DINO	23.6	12.2	12.8	20.0	9.4	10.2	22.7	12.2	12.7	19.2	9.3	10.0
CutS3D (Ours)	DiffNCuts	24.3	12.2	13.0	20.6	9.3	10.3	23.9	12.2	13.0	20.1	9.2	10.2

Table 1. **Unsupervised Instance Segmentation.** Our model is able to outperform the previous state-of-the-art in a zero-shot setting on COCO with DINO-based and DiffNCuts-based pseudo ground truth. CutS3D (Ours), CutLER and CuVLER and ProMerge+ are all evaluated zero-shot. * Results obtained using official checkpoint.

Spatial Confidence Soft Target Loss. To directly incorporate the pseudo-mask quality into the learning signal, we propose to modify the loss of our CAD. In CuVLER, Arica et al. [1] propose a soft target loss, which essentially re-weights the loss for an entire mask by a scalar. Since our Spatial Confidence is computed for each region in the mask individually, we use it to introduce a Spatial Confidence Soft Target loss. Instead of multiplying the full mask loss by a scalar, we re-weight the loss for each mask region individually with its confidence score, performing a much more targeted operation to incorporate patch-level confidence. We utilize a Cascade Mask R-CNN [4] as our CAD, which computes a binary cross-entropy (BCE) loss on the pseudo mask. For our Spatial Confidence Soft Target Loss, we re-weight each part of the loss using

$$L_{\text{mask}} = \sum_{(i,j)} \text{SC}_{i,j} \cdot \text{BCE}(\hat{M}_{i,j}, M_{i,j}) \quad (6)$$

for each mask, with $\text{BCE}(\hat{M}_{i,j}, M_{i,j})$ being the binary cross entropy, \hat{M} and M being the predicted and target pseudo-mask, and $\text{SC}_{i,j}$ being the Spatial Confidence at i, j . In this way, the confidence of LocalCut in its pseudo-masks is more precisely reflected in the learning signal for the CAD. It is important to note that all loss values outside the confidence map are left unchanged, i.e. we set $\text{SC}_{i,j} = 1$.

4. Experiments

Experiment Setup. Following Wang et al. [47], we extract pseudo masks on the entire training split of ImageNet [33] (IN1K), consisting of roughly 1.3 million natural images. Each image is resized into 480×480 pixels and fed into the feature encoder \mathcal{F} . We experiment with two different encoders: A DINO ViT-B/8 [6] and a DiffNCuts ViT-S/8 [28], which is a DINO finetuned with differentiable NCut. Our approach also uses NCut for the initial semantic cut, making the network a natural choice. Following, we adopt the choice of training a Cascade Mask R-CNN [4] with Spatial Confidence and DropLoss [47] on the initial IN1K CutS3D

pseudo masks. We keep the settings from CutLER largely the same and report hyperparameter configurations in the supplementary. After training on the pseudo-masks, we perform one round of self-training [47] on the predictions from the first trained model. We evaluate this model in our zero-shot evaluation settings on a variety of natural image datasets. In additional, we experiment with further training in-domain, as first proposed by Arica et al. [1]. For this, we perform another round of self-training, but on COCO train2017 [27]. For a fair evaluation, we only compare this model against others which have conducted further self-training on the target domain.

Datasets. We evaluate our approach on an extensive suite of benchmarks of natural image datasets, namely COCO val2017 [27], COCO20K [27] and LVIS [16], Pascal VOC [12], Objects365 [36], KITTI [13] and OpenImages [25]. We consider both object detection and instance segmentation evaluations where annotations are given.

4.1. Unsupervised Instance Segmentation

We first evaluate our IN1K-trained models on unsupervised instance segmentation in a zero-shot setting. Table 1 shows comparison of our model on COCO20K and COCO val2017 [27] to the best performing models of many recent approaches for zero-shot unsupervised instance segmentation. We report results for our model trained on pseudo-masks extracted from DINO features as well as DiffNCut features. For both settings, we find that we outperforms the previous state-of-the-art by notable margins, especially when pseudo-masks are generated with DiffNCuts [28]. Our best model improves by **+0.4 AP^{mask}** on COCO val2017 and **+0.3 AP^{mask}** on COCO20K versus the best competitor. Our approach also outperforms the CutLER baseline despite it being further self-trained.

4.2. Unsupervised Object Detection

We further evaluate zero-shot object detection on a range of datasets. In Table 2, we report the performance of our model trained on our pseudo-masks extracted with the DiffNCuts

Method	Average		COCOval2017		COCO20K		VOC		Objects365		OpenImages		KITTI		LVIS	
	AP ₅₀ ^{box}	AP ^{box}	AP ₅₀ ^{box}	AP ^{box}	AP ₅₀ ^{box}	AP ^{box}	AP ₅₀ ^{box}	AP ^{box}	AP ₅₀ ^{box}	AP ^{box}	AP ₅₀ ^{box}	AP ^{box}	AP ₅₀ ^{box}	AP ^{box}	AP ₅₀ ^{box}	AP ^{box}
CuVLER [1]	21.0	11.3	23.0	12.6	23.5	12.7	39.4	22.3	21.6	10.9	19.6	11.6	11.8	4.6	8.5	4.5
CutLER [47]	20.9	11.3	21.9	12.5	22.4	12.5	36.9	20.2	21.6	11.4	17.3	9.7	18.4	8.5	8.4	4.5
CutS3D (Ours)	22.3	11.7	23.9	13.0	24.3	13.0	40.6	21.4	22.3	11.4	18.1	10.0	18.7	8.7	8.5	4.5

Table 2. **Zero-Shot Unsupervised Object Detection.** Our approach trained with DiffNCuts-based pseudo-masks outperforms competitors on multiple benchmarks, despite CutLER being further self-trained and CuVLER using a 6-model ensemble for pseudo-masks generation.

Dataset	COCOval2017		COCO20K		LVIS	
	AP ₅₀ ^{mask}	AP ^{mask}	AP ₅₀ ^{mask}	AP ^{mask}	AP ₅₀ ^{mask}	AP ^{mask}
CuVLER [1]	20.4	10.4	21.6	10.7	7.2	3.8
CutS3D	20.4	11.1	22.4	11.4	8.4	5.6

Table 3. **In-Domain Self-Training.** Our method is able to outperform CuVLER after both models have been further self-trained on the COCO target domain.

backbone. We show that our model improves upon the baseline, CutLER [47], on average by **+1.3 AP₅₀^{box}** and **+0.4 AP^{box}** across all datasets, even though CutLER has been trained with additional self-training, showing the efficiency of our method. Similar to zero-shot unsupervised instance segmentation, our method also outperforms the best competing method, CuVLER [1], on most benchmarks. Notably, this is the case despite CuVLER using an ensemble of 6 different DINO ViTs for pseudo-mask extraction, while our method leverages only one feature extractor and 3D. This also showcases the effectiveness of 3D information in comparison to additional feature extractors.

4.3. In-Domain Self-Training

Previous results were reported with models trained solely on the ImageNet domain and then evaluated on a other data domains. We also adopt the target-domain training setting from Arica et al. [1] and further self-train our model for one more round on the COCO train2017 dataset. To obtain the pseudo ground truth, we use our best zero-shot model generate pseudo masks for the COCO train2017. Table 3 compares our model to CuVLER, which has also been further self-trained on COCO. We outperform their method across all three versions of COCO. Our method improves by **+0.7 AP^{mask}** on the val2017 split and by **+0.7 AP^{mask}** on COCO20K. Most notably, our model better captures the challenging fine-grained visual concepts of the long-tail LVIS benchmark where we outperform CuVLER by **+1.8 AP^{mask}**. This demonstrates that our zero-shot model can produce accurate masks also on datasets outside the ImageNet domain effective for domain-specific training.

5. Ablations

We ablate our proposed technical components by training the CAD on the generated IN1K pseudo-masks with DiffNCuts features and evaluating in a zero-shot manner on

Backbone	DINO[6]		DiffNCuts[28]	
	AP ₅₀ ^{mask}	AP ^{mask}	AP ₅₀ ^{mask}	AP ^{mask}
CutLER [†]	17.5	8.5	18.7	9.4
+ LocalCut (1)	17.9	8.7	18.9	9.5
+ Spatial Importance (2)	18.1	9.1	19.2	9.8
+ Spatial Confidence (3, 4, 5)	19.2	10.0	20.1	10.2

Table 4. **Effect of our contributions.** We compare our individual contributions after one round of self-training. [†]Results reproduced using the authors’ official implementation.

COCO val2017. Only for Table 4 & 6 do we conduct one round of self-training for better comparison with Table 1.

Effect Of Our Individual Contributions. We investigate the effect of our contributions across both proposed backbones. In Table 4, we sequentially add the presented technical contributions and evaluate them with our main zero-shot protocol, i.e. by training one round on pseudo-masks and then one round of self-training. As a basis, we reproduce CutLER [47] from scratch with both backbones by first generating MaskCut pseudo-masks, then training a CAD on them, followed by one round of self-training, using the official author implementation. We find that using DiffNCuts improves the purely semantics-based baseline. As can be observed, each added technical component improves our model over this baseline. A strong effect can be seen from the combination of LocalCut (1) and Spatial Importance (2), since they amplify each other: With the improved semantics achieved through Spatial Importance sharpening, LocalCut can more often identify the 3D object boundary, leading to better performance. Spatial Confidence further improves performance and we present a detailed analysis of our Spatial Confidence components in the later section.

Training Rounds. A crucial factor to our method’s effectiveness is self-training. We make similar finding as Wang et al. [47] that the CAD can extract the signal well from the pseudo-masks and refines it further with self-training. We conduct one round of self-training after the pseudo-mask training, reducing the computational overhead compared to CutLER, which conducts further self-training. We report results for the CAD trained with DINO- and DiffNCuts-based pseudo-masks for initial training and one round of self-training in Table 6.

Spatial Confidence Components Analysis. We further investigate the effect of our Spatial Confidence contributions. Therefore, we add each of the contributions that use

τ_{knn}	.1	.115	.13	α	Scalar	Spatial	SC_{ij}^{min}	.5	.67	.83	With	Without	
AP_{mask}	8.3	8.5	8.4	AP_{mask}	8.8	9.0	AP_{mask}	9.1	9.0	9.0	AP_{mask}	9.1	9.1
(a) Different values for τ_{knn} .			(b) Alpha Blending Variations.			(c) SC Lower Bound.			(d) SC Maps Mask-Alignment.				

Table 5. **Further ablations.** We explore several variations of parameters and design aspects in our contributions.

Training	Method	COCOval2017		
		AP_{50}^{mask}	AP_{75}^{mask}	AP^{mask}
Initial Pseudo-Masks	Ours (DINO)	16.4	7.5	8.2
	Ours (DiffNCut)	18.0	8.0	9.1
One-Round Self-Training	Ours (DINO)	19.2	9.3	10.0
	Ours (DiffNCut)	20.1	9.2	10.2

Table 6. **Intermediate Results after training rounds.** Zero-Shot results on COCO val2017 after training a Cascade Mask R-CNN on the initial pseudo-masks and after one round of self-training.

Confident Copy-Paste	Alpha Blend	Spatial Confidence Loss	AP^{mask}
\times	\times	\times	8.5
\checkmark	\times	\times	8.8
\checkmark	\checkmark	\times	9.0
\checkmark	\checkmark	\checkmark	9.1

Table 7. **Spatial Confidence Component Analysis.** Zero-Shot results on COCO val2017 after training the Cascade Mask R-CNN on the initial pseudo-masks, generated with Ours (DiffNCuts). We do not conduct self-training to isolate the components’ effect.

Spatial Confidence individually to our CAD. We train the model only on the initial pseudo-masks without further self-training to best surface the effect, since self-training has the potential to blur the performance differences. As shown in Table 7, selecting only confident masks for copy-paste augmentation leads to the biggest boost in performance. Adding alpha-blending with Spatial Confidence further improves results, while applying our Spatial Confidence Soft Loss further nudges up the performance even more.

Depth Sources. Recently, progress in zero-shot monocular depth estimation has led to many different models that generalize well across many domains. While some earlier approaches mix different datasets with sensor information [2, 31, 32] to train their model, more recent approaches using self-supervision [7, 41, 42] and training on synthetic depth [3, 18, 22] have also gained traction. We opt to select one depth estimator from each of these categories to evaluate their applicability to our method: ZoeDepth [2] is a finetuned MiDaS [31] on a mix of metric depth datasets, Marigold [22] is a repurposed diffusion model to learn depth from synthetic data only, and Kick, Back & Relax [41] is using self-supervision to learn depth from SlowTV videos. For each model, we predict the depth for the entire IN1K training set. We use our best-performing model configuration and DiffNCuts as the feature extractor for the pseudo-masks, only varying the depth source for the experiment. Using the pseudo-masks, we train the CAD with all contributions on the pseudo-masks without fur-

Method	Trained with	AP_{50}^{mask}	AP^{mask}
ZoeDepth [2]	Sensor Depth	18.0	9.1
Marigold [22]	Synthetic Depth	17.8	8.9
Kick Back & Relax [41]	Self-Supervision	17.8	9.1

Table 8. **Depth Estimators.** We ablate different depth sources.

ther self-training and report the zero-shot results on COCO val2017 in Table 8. We observe that all depth estimators are equally suited for our method. This supported by the qualitative depth visualizations of the predicted depth, which we compare as part of the supplementary.

Further Ablations. We further investigate the aspects of our contribution design choices. Table 5a shows variations for τ_{knn} in LocalCut, the CAD is trained on the pseudo-masks without Spatial Confidence to isolate the parameters effect. In Table 5b, we experiment using the average confidence as α instead of the Spatial Confidence maps. We do not use the Spatial Confidence loss to clearly show the effect. We also experiment with a confidence lower bound in Table 5c, and with aligning the patchy Spatial Confidence maps to the pseudo-mask borders. As shown in Table 5d, we find this alignment is not necessary performance-wise.

6. Limitations

Even when 3D information is available, our approach can struggle to extract accurate masks, if adjacent instances with similar semantics lack discernible 3D boundaries. Further, while we observe that our model can improve previous baselines for detection of smaller objects, this still remains an issue in unsupervised instance segmentation. We show a selection of failure cases in the supplementary. Further, our method’s application is limited when 3D information cannot be obtained, as it is the case for some medical data.

7. Summary

We have introduced CutS3D, a novel approach for leveraging 3D information for 2D unsupervised instance segmentation. With our LocalCut, we cut along the actual 3D boundaries of instances, while Spatial Importance Sharpening enables clearer semantic relations in areas of high-frequency depth changes. Further, we propose the concept of Spatial Confidence to select only high-quality masks for copy-paste augmentation, alpha-blend the pasted objects and introduce a novel Spatial Confidence Soft Target Loss. CutS3D is able to achieve improved performance across multiple natural image benchmarks, in zero-shot settings and with fur-

ther in-domain self-training. While CutS3D also improves results for in-domain training in comparison to other approaches, we believe extracting pseudo-masks directly in-domain without relying on ImageNet is a fruitful direction for further progress in the future.

References

- [1] Shahaf Arica, Or Rubin, Sapir Gershov, and Shlomi Laufer. Cuvler: Enhanced unsupervised object discoveries through exhaustive self-supervised transformers. In *Proceedings of the IEEE/CVF Conference on Computer Vision and Pattern Recognition*, pages 23105–23114, 2024. 2, 6, 7
- [2] Shariq Farooq Bhat, Reiner Birkl, Diana Wofk, Peter Wonka, and Matthias Müller. Zoedepth: Zero-shot transfer by combining relative and metric depth. *arXiv preprint arXiv:2302.12288*, 2023. 3, 8
- [3] Aleksei Bochkovskii, Amaël Delaunoy, Hugo Germain, Marcel Santos, Yichao Zhou, Stephan R Richter, and Vladlen Koltun. Depth pro: Sharp monocular metric depth in less than a second. *arXiv preprint arXiv:2410.02073*, 2024. 8
- [4] Zhaowei Cai and Nuno Vasconcelos. Cascade r-cnn: High quality object detection and instance segmentation. *IEEE transactions on pattern analysis and machine intelligence*, 43(5):1483–1498, 2019. 1, 6
- [5] Mathilde Caron, Ishan Misra, Julien Mairal, Priya Goyal, Piotr Bojanowski, and Armand Joulin. Unsupervised learning of visual features by contrasting cluster assignments. *Advances in neural information processing systems*, 33:9912–9924, 2020. 2
- [6] Mathilde Caron, Hugo Touvron, Ishan Misra, Hervé Jégou, Julien Mairal, Piotr Bojanowski, and Armand Joulin. Emerging properties in self-supervised vision transformers. In *Proceedings of the IEEE/CVF international conference on computer vision*, pages 9650–9660, 2021. 2, 6, 7
- [7] Aurélien Cecille, Stefan Duffner, Franck Davoine, Thibault Neveu, and Rémi Agier. Groco: Ground constraint for metric self-supervised monocular depth. In *European Conference on Computer Vision (ECCV)*, 2024. 8
- [8] Kai Chen, Jiangmiao Pang, Jiaqi Wang, Yu Xiong, Xiaoxiao Li, Shuyang Sun, Wansen Feng, Ziwei Liu, Jianping Shi, Wanli Ouyang, et al. Hybrid task cascade for instance segmentation. In *Proceedings of the IEEE/CVF conference on computer vision and pattern recognition*, pages 4974–4983, 2019. 1
- [9] Bowen Cheng, Ishan Misra, Alexander G Schwing, Alexander Kirillov, and Rohit Girdhar. Masked-attention mask transformer for universal image segmentation. In *Proceedings of the IEEE/CVF conference on computer vision and pattern recognition*, pages 1290–1299, 2022. 1
- [10] Efim A Dinic. Algorithm for solution of a problem of maximum flow in networks with power estimation. In *Soviet Math. Doklady*, pages 1277–1280, 1970. 3
- [11] Alexey Dosovitskiy. An image is worth 16x16 words: Transformers for image recognition at scale. *arXiv preprint arXiv:2010.11929*, 2020. 2
- [12] Mark Everingham, Luc Van Gool, Christopher KI Williams, John Winn, and Andrew Zisserman. The pascal visual object classes (voc) challenge. *International journal of computer vision*, 88:303–338, 2010. 6
- [13] Andreas Geiger, Philip Lenz, Christoph Stiller, and Raquel Urtasun. Vision meets robotics: The kitti dataset. *The International Journal of Robotics Research*, 32(11):1231–1237, 2013. 6
- [14] Golnaz Ghiasi, Yin Cui, Aravind Srinivas, Rui Qian, Tsung-Yi Lin, Ekin D Cubuk, Quoc V Le, and Barret Zoph. Simple copy-paste is a strong data augmentation method for instance segmentation. In *Proceedings of the IEEE/CVF conference on computer vision and pattern recognition*, pages 2918–2928, 2021. 5
- [15] Aleksey Golovinskiy and Thomas Funkhouser. Min-cut based segmentation of point clouds. In *2009 IEEE 12th International Conference on Computer Vision Workshops, ICCV Workshops*, pages 39–46. IEEE, 2009. 3
- [16] Agrim Gupta, Piotr Dollar, and Ross Girshick. Lvis: A dataset for large vocabulary instance segmentation. In *Proceedings of the IEEE/CVF conference on computer vision and pattern recognition*, pages 5356–5364, 2019. 6
- [17] Mark Hamilton, Zhoutong Zhang, Bharath Hariharan, Noah Snavely, and William T Freeman. Unsupervised semantic segmentation by distilling feature correspondences. *arXiv preprint arXiv:2203.08414*, 2022. 2
- [18] Jing He, Haodong Li, Wei Yin, Yixun Liang, Leheng Li, Kaiqiang Zhou, Hongbo Liu, Bingbing Liu, and Yingcong Chen. Lotus: Diffusion-based visual foundation model for high-quality dense prediction. *arXiv preprint arXiv:2409.18124*, 2024. 8
- [19] Kaiming He, Georgia Gkioxari, Piotr Dollár, and Ross Girshick. Mask r-cnn. In *Proceedings of the IEEE international conference on computer vision*, pages 2961–2969, 2017. 1, 2
- [20] Kaiming He, Haoqi Fan, Yuxin Wu, Saining Xie, and Ross Girshick. Momentum contrast for unsupervised visual representation learning. In *Proceedings of the IEEE/CVF conference on computer vision and pattern recognition*, pages 9729–9738, 2020. 2
- [21] Ronghang Hu, Piotr Dollár, Kaiming He, Trevor Darrell, and Ross Girshick. Learning to segment every thing. In *Proceedings of the IEEE conference on computer vision and pattern recognition*, pages 4233–4241, 2018. 1
- [22] Bingxin Ke, Anton Obukhov, Shengyu Huang, Nando Metzger, Rodrigo Caye Daudt, and Konrad Schindler. Repurposing diffusion-based image generators for monocular depth estimation. In *Proceedings of the IEEE/CVF Conference on Computer Vision and Pattern Recognition*, pages 9492–9502, 2024. 8
- [23] Chanyoung Kim, Woojung Han, Dayun Ju, and Seong Jae Hwang. Eagle: Eigen aggregation learning for object-centric unsupervised semantic segmentation. In *Proceedings of the IEEE/CVF Conference on Computer Vision and Pattern Recognition*, pages 3523–3533, 2024. 2
- [24] Philipp Krähenbühl and Vladlen Koltun. Efficient inference in fully connected crfs with gaussian edge potentials. *Ad-*

- vances in neural information processing systems, 24, 2011. 4
- [25] Alina Kuznetsova, Hassan Rom, Neil Alldrin, Jasper Uijlings, Ivan Krasin, Jordi Pont-Tuset, Shahab Kamali, Stefan Popov, Matteo Mallocci, Alexander Kolesnikov, Tom Duerig, and Vittorio Ferrari. The open images dataset v4: Unified image classification, object detection, and visual relationship detection at scale. *IJCV*, 2020. 6
- [26] Dylan Li and Gyungin Shin. Promerge: Prompt and merge for unsupervised instance segmentation. In *European Conference on Computer Vision (ECCV)*, 2024. 2, 6
- [27] Tsung-Yi Lin, Michael Maire, Serge Belongie, James Hays, Pietro Perona, Deva Ramanan, Piotr Dollár, and C Lawrence Zitnick. Microsoft coco: Common objects in context. In *Computer Vision—ECCV 2014: 13th European Conference, Zurich, Switzerland, September 6–12, 2014, Proceedings, Part V 13*, pages 740–755. Springer, 2014. 1, 6
- [28] Yanbin Liu and Stephen Gould. Unsupervised dense prediction using differentiable normalized cuts. In *ECCV*, 2024. 2, 6, 7
- [29] Thomas Luft, Carsten Colditz, and Oliver Deussen. Image enhancement by unsharp masking the depth buffer. *ACM Transactions on Graphics (ToG)*, 25(3):1206–1213, 2006. 4
- [30] Maxime Oquab, Timothée Darcet, Théo Moutakanni, Huy Vo, Marc Szafranec, Vasil Khalidov, Pierre Fernandez, Daniel Haziza, Francisco Massa, Alaaeldin El-Nouby, et al. Dinov2: Learning robust visual features without supervision. *arXiv preprint arXiv:2304.07193*, 2023. 2
- [31] René Ranftl, Katrin Lasinger, David Hafner, Konrad Schindler, and Vladlen Koltun. Towards robust monocular depth estimation: Mixing datasets for zero-shot cross-dataset transfer. *IEEE transactions on pattern analysis and machine intelligence*, 44(3):1623–1637, 2020. 8
- [32] René Ranftl, Katrin Lasinger, David Hafner, Konrad Schindler, and Vladlen Koltun. Towards robust monocular depth estimation: Mixing datasets for zero-shot cross-dataset transfer. *IEEE transactions on pattern analysis and machine intelligence*, 44(3):1623–1637, 2020. 8
- [33] Olga Russakovsky, Jia Deng, Hao Su, Jonathan Krause, Sanjeev Satheesh, Sean Ma, Zhiheng Huang, Andrej Karpathy, Aditya Khosla, Michael Bernstein, et al. Imagenet large scale visual recognition challenge. *International journal of computer vision*, 115:211–252, 2015. 6
- [34] Alexandre Sablayrolles, Matthijs Douze, Cordelia Schmid, and Hervé Jégou. Spreading vectors for similarity search. In *ICLR 2019-7th International Conference on Learning Representations*, pages 1–13, 2019. 2
- [35] Hyun Seok Seong, WonJun Moon, SuBeen Lee, and Jae-Pil Heo. Leveraging hidden positives for unsupervised semantic segmentation. In *Proceedings of the IEEE/CVF conference on computer vision and pattern recognition*, pages 19540–19549, 2023. 2
- [36] Shuai Shao, Zeming Li, Tianyuan Zhang, Chao Peng, Gang Yu, Xiangyu Zhang, Jing Li, and Jian Sun. Objects365: A large-scale, high-quality dataset for object detection. In *Proceedings of the IEEE/CVF international conference on computer vision*, pages 8430–8439, 2019. 6
- [37] Xing Shen, Jirui Yang, Chunbo Wei, Bing Deng, Jianqiang Huang, Xian-Sheng Hua, Xiaoliang Cheng, and Kewei Liang. Dct-mask: Discrete cosine transform mask representation for instance segmentation. In *Proceedings of the IEEE/CVF conference on computer vision and pattern recognition*, pages 8720–8729, 2021. 1
- [38] Jianbo Shi and Jitendra Malik. Normalized cuts and image segmentation. *IEEE Transactions on pattern analysis and machine intelligence*, 22(8):888–905, 2000. 3, 4
- [39] Leon Sick, Dominik Engel, Pedro Hermosilla, and Timo Ropinski. Unsupervised semantic segmentation through depth-guided feature correlation and sampling. In *Proceedings of the IEEE/CVF Conference on Computer Vision and Pattern Recognition*, pages 3637–3646, 2024. 1, 2
- [40] Oriane Siméoni, Gilles Puy, Huy V. Vo, Simon Roburin, Spyros Gidaris, Andrei Bursuc, Patrick Pérez, Renaud Marlet, and Jean Ponce. Localizing objects with self-supervised transformers and no labels. 2021. 2, 6
- [41] Jaime Spencer, Chris Russell, Simon Hadfield, and Richard Bowden. Kick back & relax: Learning to reconstruct the world by watching slowtv. In *Proceedings of the IEEE/CVF International Conference on Computer Vision*, pages 15768–15779, 2023. 8
- [42] Jaime Spencer, Chris Russell, Simon Hadfield, and Richard Bowden. Kick back & relax++: Scaling beyond ground-truth depth with slowtv & cribstv. *arXiv preprint arXiv:2403.01569*, 2024. 8
- [43] Wouter Van Gansbeke, Simon Vandenhende, and Luc Van Gool. Discovering object masks with transformers for unsupervised semantic segmentation. *arXiv preprint arXiv:2206.06363*, 2022. 2, 6
- [44] Xinlong Wang, Rufeng Zhang, Chunhua Shen, Tao Kong, and Lei Li. Dense contrastive learning for self-supervised visual pre-training. In *Proceedings of the IEEE/CVF conference on computer vision and pattern recognition*, pages 3024–3033, 2021. 2
- [45] Xinlong Wang, Rufeng Zhang, Chunhua Shen, Tao Kong, and Lei Li. Solo: A simple framework for instance segmentation. *IEEE transactions on pattern analysis and machine intelligence*, 44(11):8587–8601, 2021. 2
- [46] Xinlong Wang, Zhiding Yu, Shalini De Mello, Jan Kautz, Anima Anandkumar, Chunhua Shen, and Jose M Alvarez. Freesolo: Learning to segment objects without annotations. In *Proceedings of the IEEE/CVF conference on computer vision and pattern recognition*, pages 14176–14186, 2022. 2, 6
- [47] Xudong Wang, Rohit Girdhar, Stella X Yu, and Ishan Misra. Cut and learn for unsupervised object detection and instance segmentation. In *Proceedings of the IEEE/CVF conference on computer vision and pattern recognition*, pages 3124–3134, 2023. 1, 2, 3, 4, 5, 6, 7
- [48] Yangtao Wang, Xi Shen, Yuan Yuan, Yuming Du, Maomao Li, Shell Xu Hu, James L Crowley, and Dominique Vaufreydaz. Tokencut: Segmenting objects in images and videos with self-supervised transformer and normalized cut. *IEEE transactions on pattern analysis and machine intelligence*, 2023. 2

- [49] Rufeng Zhang, Zhi Tian, Chunhua Shen, Mingyu You, and Youliang Yan. Mask encoding for single shot instance segmentation. In *Proceedings of the IEEE/CVF conference on computer vision and pattern recognition*, pages 10226–10235, 2020. 1
- [50] Jinghao Zhou, Chen Wei, Huiyu Wang, Wei Shen, Cihang Xie, Alan Yuille, and Tao Kong. Image bert pre-training with online tokenizer. In *International Conference on Learning Representations*. 2